Chapter 4
The Influence of Stray Current on the Maturity Level of Cement-Based Materials

A. Susanto, Dessi A. Koleva, and Klaas van Breugel

Abstract This work reports on the influence of stray current on the development of mechanical and electrical properties of mortar specimens in sealed and water-submerged conditions. In the absence of concentration gradients with external environment (sealed conditions) or in their presence (submerged conditions), compressive strength and electrical resistivity change due to: cement hydration alone; cement hydration, affected by diffusion (including leaching-out); or cement hydration, simultaneously influenced by diffusion and migration. The results are compared to equally conditioned control specimens, where stray current was not involved.

In view of material properties development over time, the ageing factor in relevant exposure conditions is addressed, considering reported approaches for its determination. Through implementing existing methodology and based on experimentally derived electrical resistivity values, the ageing factor for sealed conditions was determined. The apparent diffusion coefficients were calculated based on ageing factors and reported relationships, reflecting the effect of stray current on matrix diffusivity.

Two levels of electrical current density, 100 mA/m^2 and 1 A/m^2, were employed as a simulation of stray current to 28 days-cured mortar specimens with water-to-cement ratio of 0.5 and 0.35. For the time interval of these tests of ca. 110 days, the experimental results show the positive effect of stray current on mortar specimens in sealed conditions and the negative effect for water-submerged conditions.

For sealed specimens, increase of compressive strength and electrical resistivity were recorded, more pronounced for the higher current density level of 1 A/m^2.

A. Susanto (✉) • D.A. Koleva • K. van Breugel
Faculty of Civil Engineering and Geosciences, Delft University of Technology,
Section of Materials and Environment, Stevinweg 1, 2628 CN Delft, The Netherlands
e-mail: a.susanto@tudelft.nl

L.E. Rendon Diaz Miron, D.A. Koleva (eds.), *Concrete Durability*,
DOI 10.1007/978-3-319-55463-1_4

This effect was irrespective of w/c ratio. Increased electrical resistivity and superior performance overall, would determine improved material properties in terms of reduced permeability and diffusivity of the matrix. The results show that for sealed specimens in stray current conditions, the apparent diffusion coefficient was reduced, the effect being more pronounced for the higher current density level of $1A/m^2$ and (logically) for the lower w/c ratio of 0.35.

In contrast, for water-submerged mortar, a reversed trend of material behavior was observed i.e. reduced mechanical and electrical properties were recorded to be resulting from stray current flow.

Defining a threshold for a positive or negative stray current effect was not possible to be determined from this work. Higher current density levels in varying external environment are necessary to be studied, in order to potentially define such threshold. However, the results clearly show that stray current affects the development of material properties of cement-based materials, an aspect that is rarely considered in the current practice.

Keywords Aging factor • Cement-based materials • Electrical resistivity • Stray current

4.1 General Introduction

The aspects of concrete structures' durability have always been a main concern for the engineering practice. Numerous methods have been proposed to predict service life and reliably foresee structures' performance within their designed life span. One of the important parameters, employed to predict service life, is the so-called "aging factor." The aging factor depends on variables such as the type of cement used and the mix proportion, as well as environmental exposure conditions. All these are further commonly used to predict concrete diffusivity, which is of great significance with respect to durability-related properties of concrete and cement-based materials overall.

Several approaches are known to determine the aging factor of cement-based materials and link these outcomes with concrete diffusivity. Among these, common techniques include natural diffusion tests and accelerated tests, involving the application of electrical current (or voltage) [1–6]. Numerous studies report on different methods for determining concrete diffusivity and chloride transport in cement-based materials [1–10]. Some of these focus on the relationship between nonsteady state diffusion, nonsteady state migration, and steady-state migration tests, referring to test setup as specified in NT Build 443, NT Build 492, and NT Build 355 [5, 7–9]. Other approaches link electrical properties and maturity levels of cement-based materials with diffusivity and aging factors, respectively [11–15].

Determination of water and chloride ions transport in porous medium as concrete, properties as diffusivity, electrical resistivity, maturity, etc., are directly linked to durability, service life, and the aging factor, respectively, of cement-based materials. The transport of fluids and ionic species occurs according to four transport

mechanisms such as diffusion due to a concentration gradient, migration due to an electrical potential gradient, permeation due to a pressure gradient, and absorption due to capillary action [6, 16, 17]. These mechanisms are strongly related to and determine the microstructural properties of cement-based materials. Microstructural properties, in turn, determine the global performance of cement-based structures. However, cement-based microstructure development, as governed by cement hydration, would be affected by the abovementioned transport mechanisms, which will progress with various rates if migration i.e. electrical current is involved. Therefore, it is important to clearly differentiate the effect of migration in conditions where ion and water transport are limited to the internal pore water only, from these, where transport mechanisms are largely depended on environmental exposure and conditions. In this work, global performance and properties of sealed and water submerged mortar specimens (compressive strength and electrical resistivity) were derived in rest (control) conditions and in conditions of applied electrical field (stray current). The objective was to clearly differentiate material properties development due to cement hydration only from properties development, additionally affected by altered diffusion and migration, as within stray current conditions. The technical background in the following section summarises the relevant state-of-the-art on main points for material properties evaluation, together with analytical models for deriving parameters of interest (e.g. ageing factor and apparent diffusion coefficients), linking these to the results and discussion in this work.

4.2 Technical Background

4.2.1 Transport Mechanisms and Diffusion Coefficients

4.2.1.1 Diffusion Tests

The natural diffusion test is commonly used to simulate the natural process of chloride transport in concrete as a porous medium. The method is based on diffusion cell tests and immersion tests, employing chloride concentration simulating sea water, i.e., approximately 3.5 wt% [6]. The immersion tests are essentially an immersion of the specimens in a solution, containing a constant chloride concentration. The chloride penetration over time is recorded by grinding the specimen and analyzing the chloride concentration in a direction from the exposed surface towards the bulk material. The result is obtaining a chloride profile after a certain time of immersion. Next, the apparent chloride diffusion coefficient is determined by curve-fitting of the measured chloride profile to the error function in the analytical solution of Flick's second law (Eq. 4.1). The results strongly depend on the immersion period and the chloride concentration in the external bulk solution [6]. In contrast, for the diffusion cell test following NT BUILD 443 [7], where relevant considerations and experimental setup are described in detail, a water-saturated

concrete specimen is exposed on one plane surface only to sodium chloride solution (chloride concentration in the range of 3–20%). The chloride content of the cement-based matrix at certain exposure time-intervals is determined within thin layers, ground off in parallel to the exposed face of the specimen. According to NT BUILD 443, the diffusion coefficient can be calculated as follows:

$$C\left(x,t\right) = C_{\mathrm{s}} - \left(C_{\mathrm{s}} - C_{\mathrm{i}}\right).\mathrm{erf}\left(\frac{x}{\sqrt{4.D_{\mathrm{e}}.t}}\right) \tag{4.1}$$

where $C(x,t)$ is the chloride concentration, measured at the depth x at exposure time t (mass %), C_{s} is the boundary condition at the exposed surface (mass %), C_{i} is the initial chloride concentration measured on the concrete slice boundary condition at the exposed surface (mass %), x is the depth below the exposed surface (m), D_{e} is the effective chloride diffusion coefficient ($\mathrm{m^2/s}$), t is the exposure time, and erf is the standard error function that can be expressed as below:

$$\mathrm{erf}\left(z\right) = \frac{2}{\sqrt{\pi}}\int_{z}^{0}\exp\left(-y^2\right)\mathrm{d}y \tag{4.2}$$

Except the above considerations on determining chloride diffusion coefficients and concrete diffusivity, respectively, the application of chloride diffusion tests has also been reported as an aging factor determination approach [1, 10, 18]. The main aspects of this approach are as follows: Fick's second law (Eq. 4.1) is commonly used to calculate chloride profiles at a certain depth and time. In order to predict service life of concrete structures, the effective chloride diffusion coefficient (D_{e}) in Eq. (4.1) is modified and governed by the following equation [10, 19]:

$$D\left(t\right) = D_{\mathrm{o}}\left(\frac{t}{t_{\mathrm{o}}}\right)^{-n} \tag{4.3}$$

where D_{o} is the chloride diffusion coefficient at the reference time t_{o} (usually 28 days age), n is the aging factor ($0 \leq n \leq 1$), and t is the age of concrete.

4.2.1.2 Migration Tests

Since natural diffusion is a very slow process, accelerated diffusion test methods are also used, e.g., the rapid chloride migration (RCM) test where chloride ions migration, as a predominant transport mechanism due to the applied voltage in the RCM cell, is in parallel with diffusion of chloride ions (details of the RCM tests are as described in [1, 10] and not subject to elaboration here). Similarly to diffusion tests,

the outcomes for concrete diffusivity and diffusion coefficients derived from migration tests can be employed to determine the aging factor for the tested concrete specimens. This approach employs the Nernst-Einstein equation, according to which the chloride diffusion coefficient for a porous material (as concrete) is inversely proportional to the electrical resistivity of this material [20]:

$$D_{\mathrm{cl}} = \frac{K}{\rho}, \text{ with } K = \frac{R.T}{z^2.F^2}\frac{t_{\mathrm{cl}}}{\gamma_{\mathrm{i}}.c_{\mathrm{i}}} \tag{4.4}$$

where D_{cl} is the diffusivity for chloride ions, R is the gas constant, T is the absolute temperature, z is the ionic valence, F is the Faraday constant, t_{i} is the transfer number of the chloride ions, γ_{i} is the activity coefficient for chloride ions, c_{i} is the chloride ions concentration in the pore water, and ρ is the electrical resistivity.

Determination of the aging factor via records of electrical resistivity development of cement-based materials (discussed further below), using the above approach has also been reported [17–19]. Following Eqs. (4.2) and (4.3), mathematical expression similar to Eq. (4.3) can be obtained, but already introducing the aging factor "***q***" as follows [10, 21]:

$$\rho(t) = \rho_{\mathrm{o}}\left(\frac{t}{t_{\mathrm{o}}}\right)^{+q} \tag{4.5}$$

$$\text{with } q = 0.798n - 0.0072 \approx 0.8n \tag{4.6}$$

The present state-of-the-art reports aging factor values derived by RCM in the range of 0.178 to 0.65 for CEM I 42.5 [22–26]. This range is in line with values determined by diffusion tests in the range of 0.218 to 0.701 [21, 23]. The range of these values are more or less in the order of aging factor values, as determined through other methods, e.g., via recorded electrical resistivity, a commonly used approach which is briefly introduced in what follows.

More recently, the determination of the aging factor of cement-based materials, based on derived electrical resistivity values (Eq. 4.4 above), was also suggested, reporting values in the range of 0.09 to 0.35 for CEM I 42.5 [11–13]. These are also more or less in line with values, recorded through diffusion or migration tests. Hence, determination of the aging factor based on electrical resistivity values is another suitable approach [11, 14]. However, the accuracy of resistivity determination would depend on the chosen method. This will affect the derived aging factor, respectively.

A brief summary of the most frequently used methods for measuring electrical resistivity of cement-based materials, as well as the approach to maturity levels' determination, is presented in what follows.

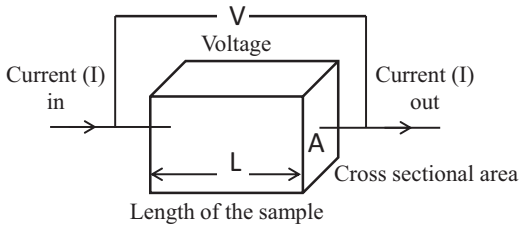

Fig. 4.1 Electrical resistivity measurement by two probes method

4.2.2 Electrical Properties and Maturity Levels

4.2.2.1 Electrical Resistivity

Monitoring electrical resistivity, a parameter directly linked to maturity of cement-based materials and also related to diffusivity, has been suggested as a convenient and nondestructive technique to assess concrete durability. Electrical resistivity of cement-based materials can be measured following various setups, review of which is not subject to this chapter and can be found described in detail in [27, 28, 29]. The general approach is to record resistance values, by applying an alternating current through a cross section of the specimens, and the resulting output of voltage (or vice versa). Basically the resistance R of a specimen is determined by Ohm's law, $R = V/I$ where V is the electrical potential (in voltage) and I is the applied current (in Ampere).

4.2.2.2 Methods for Deriving Electrical Resistivity

The manner of measuring resistivity values can be different, e.g., two probes measurements, four probes measurements (Wenner configuration), involving the rebar network as one electrode, etc., are generally used.

The two-probe measurement is the simplest method of measuring electrical resistivity – a schematic illustration is presented in Fig. 4.1. In this method, alternating current is applied to the specimens via metal plates of surface area A, equal to the sides (cross-sections) of the specimens (Fig. 4.1). The electrical potential across the specimens is measured and the electrical resistivity is calculated using the following equation:

$$\rho = \frac{RA}{l} \tag{4.7}$$

where ρ is the electrical resistivity of the sample (in Ohm.m), R is the resistance (in Ohm), A is the cross-section of the sample (in m^2), and l is the length of the sample (in m).

The two-probe method is largely used for lab conditions, due to simplicity for lab tests, but also because of the possibility to precisely define geometrical constants and minimize other contributing factors within measurements. For example, the two

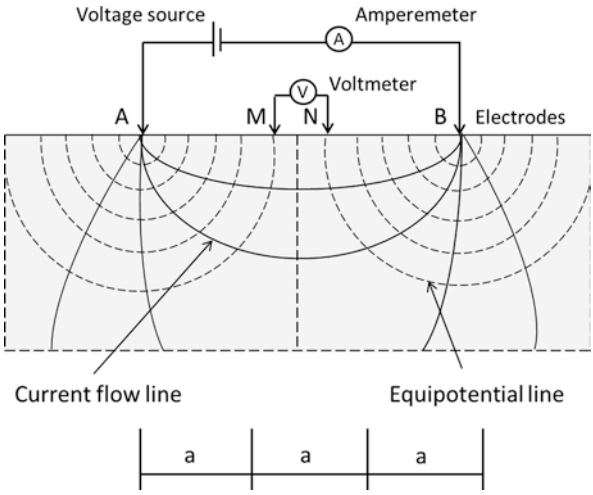

Fig. 4.2 Four electrodes configuration according to Wenner [30]

probe method can be executed at constant relative humidity or in sealed conditions, can overcome gradients of humidity or foreign resistance contribution (due to varying concrete cover thickness for example), and can be employed on specimens, which are further used for other tests (e.g., compressive strength).

The second method to measure electrical resistivity of concrete is the four probes measurement, which is developed from geophysical surveying to overcome many of the difficulties/limitation of the two-probe/point method. This method has been used for determining soil resistivity [30] and was applied to concrete structures by Stratfull [31], Naish et al. [32], and Millard [33]. The four-probe measurement is based on the so-called Wenner configuration. The method is largely applied for field tests of concrete and reinforced concrete structures, by using a portable (Wenner probe) device.

According to Wenner, the four electrodes are aligned with the same distance as illustrated in Fig. 4.2. The electrical current is "injected" via the outer electrodes (i.e., electrodes A and B), whereas the electrical potential is measured between the inner electrodes (i.e., electrodes M and N).

The electrical potentials at any nearby surface point are affected by the current flow at both current electrodes A and B (I_A and I_B). The electrical potential due to I_A at point M for example (i.e., V_{MA} and V_{MB}) can be presented as follow [30, 34]:

$$V_M = V_{MA} + V_{MB} \tag{4.8}$$

$$\text{with } V_{MA} = \frac{I\rho}{2\pi r_{MA}} \text{ and } V_{MB} = -\frac{I\rho}{2\pi r_{MB}}. \tag{4.9}$$

where V_M is the electrical potential at point M (in Volt), V_{MA} is the electrical potential between point M and point A, V_{MB} is the electrical potential between point M and point B, I is the electrical current (in Ampere), ρ is the electrical resistivity (Ohm. m), r_{MA} is the distance between point M and point A, and r_{MB} is the distance between point M and point B.

Following Eqs. (4.8) and (4.9), the resulting voltage at point M is:

$$V_{\mathrm{M}} = \frac{I\rho}{2\pi}\left(\frac{1}{r_{\mathrm{MA}}} - \frac{1}{r_{\mathrm{MB}}}\right) \tag{4.10}$$

Similarly, the electrical potential due to I_{B} at point N can be obtained as follows:

$$V_{\mathrm{N}} = V_{\mathrm{NA}} + V_{\mathrm{NB}} \tag{4.11}$$

$$\text{with } V_{\mathrm{NA}} = \frac{I\rho}{2\pi r_{\mathrm{NA}}} \text{ and } V_{\mathrm{NB}} = -\frac{I\rho}{2\pi r_{\mathrm{NB}}} \tag{4.12}$$

finally at point N:

$$V_{\mathrm{N}} = \frac{I\rho}{2\pi}\left(\frac{1}{r_{\mathrm{NA}}} - \frac{1}{r_{\mathrm{NB}}}\right) \tag{4.13}$$

where V_{N} is the electrical potential at point N (Volt), V_{NA} is the electrical potential between point N and point A, V_{NB} is the electrical potential between point N and point B, I is the electrical current (in Ampere), ρ is the electrical resistivity (Ohm. m), r_{NA} is the distance between point M and point A, and r_{NB} is the distance between point M and point B.

It should be noted that the opposite sign of electrical potential (V_{MA} positive, V_{MB} negative andV_{NA} positive, V_{NB} negative) is attributed to the reversed direction of electrical current flow. The difference of electrical potential between V_{N} and V_{M} can be calculated using the following equation:

$$\Delta V = V_{\mathrm{M}} - V_{\mathrm{N}} = \frac{I\rho}{2\pi}\left\{\left(\frac{1}{r_{\mathrm{MA}}} - \frac{1}{r_{\mathrm{MB}}}\right) - \left(\frac{1}{r_{\mathrm{NA}}} - \frac{1}{r_{\mathrm{NB}}}\right)\right\} \tag{4.14}$$

where ΔV is the electrical potential difference between two points, i.e., V_{M} and V_{N}. Next, the apparent resistivity (ρ) is obtained by rearranging Eq. (4.14) as follows:

$$\rho = \frac{2\pi\Delta V}{I} p \tag{4.15}$$

$$\text{with } p = \frac{1}{\left\{\left(\frac{1}{r_{\mathrm{MA}}} - \frac{1}{r_{\mathrm{MB}}}\right) - \left(\frac{1}{r_{\mathrm{NA}}} - \frac{1}{r_{\mathrm{NB}}}\right)\right\}} \tag{4.16}$$

where the value of p depends on the electrode geometry.

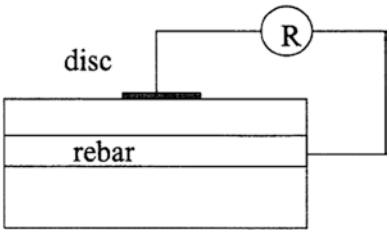

Fig. 4.3 Setup of one electrode (disc) measurement [35]

For the Wenner configuration, i.e., $r_{MA} = r_{NB} = a$ and $r_{MB} = r_{NA} = 2a$, the value of p is equal to a. Finally, the apparent resistivity in Eq. (4.15) becomes [30, 34]:

$$\rho = 2\pi a \frac{\Delta V}{I} \tag{4.17}$$

By applying Ohm's Law, Eq. (4.17) can be rewritten as:

$$\rho = 2\pi a R \tag{4.18}$$

where ρ is the electrical resistivity (in Ohm. m), a is the distance between the closest two electrodes (in m), and R is the electrical resistance (in Ohm).

The third method for measuring electrical resistivity of concrete is by involving the rebar network as one electrode [35]. This method is performed by placing a metal electrode on the concrete surface and measuring the resistance between this electrode and the reinforcement as shown in the Fig. 4.3. Basically, this method can be categorized as two-electrodes/probes type measurement. The electrical resistivity of concrete is calculated using the following equation:

$$\rho = k * R(\text{disc} - \text{bar}) \tag{4.19}$$

where ρ is electrical resistivity (in Ohm m), k is the cell constant, and R(disc-bar) is the resistance between the disc electrode and the steel bar (in Ohm).

The cell constant k is quite a complex parameter because it depends on the disc size, the concrete cover, the rebar spacing, and the rebar diameter. According to Feliu et al. [36], for disc sizes smaller than the distance to a large electrode (the rebar system), the electrical resistivity of concrete is expressed by:

$$\rho = 2 * a * R(\text{disc} - \text{bar}) \tag{4.20}$$

where a is the diameter of the disc (in m).

4.2.2.3 Maturity Method

Another method that can correlate aging phenomena and durability of cement-based materials and can be, therefore, applied for aging factors determination, is the "maturity method" [15]. The "maturity" method is a commonly used approach to predict concrete strength development, based on the temperature history of cement hydration. In general, concrete strength development is estimated by using the relationship between the maturity index and strength. The ASTM C 1074 elaborates on the procedure of this standard practice, where the maturity index can be expressed either as a temperature-time factor, using the Nurse-Saul equation, Eq. (4.21) or as the specific temperature at an equivalent age, using the Arrhenius equation, Eq. (4.22),

$$M = \sum_{t}^{0} \left(T - T_0\right) \Delta t \tag{4.21}$$

where M is the maturity index (in °C-hours or °C-days), T is the average concrete temperature (in °C), T_0 is the datum temperature (usually taken to be −10 °C), t is the elapsed time (in hours or days), and ΔT is the time interval (in hours or days).

$$t_e\left(T_r\right) = \sum_{t}^{0} e^{\frac{E}{R}\left(\frac{1}{273+T_r} - \frac{1}{273+T_c}\right)} \Delta t \tag{4.22}$$

where t_e is the equivalent age at the reference temperature (in hours), E is the apparent activation energy (in J/mol), R is the universal gas constant (in 8.314 J/mol-K), T_r is the absolute reference temperature (in Kelvin), T_c is the average concrete temperature during the time interval Δt (in Kelvin), and Δt is the chronological time interval between temperature measurements (in hours).

According to [15], concrete specimens of the same mix design and at the same maturity level have approximately the same strength, irrespective of the variance in relevant temperature and time (or their combination) in order to make up that maturity. In cement-based materials, strength increases with the progress of cement hydration. The amount of hydrated cement is determined by the duration of curing and the temperature level.

4.2.3 The Contribution of This Work

In view of the introduced technical background and state-of-the-art, this section outlines the contribution of the present work. In altered environmental conditions e.g. when electrical current flows through cement-based materials, the temperature development within cement hydration will change. A temperature increase would be expected as a consequence from ions and water migration, in addition to diffusion phenomena at interfaces e.g. pore wall/pore water. Hence, altered water and ion

transport in the cement-based bulk matrix and (re)distribution of hydration products will be at hand. If compared to control conditions, electrical current flow initially leads to accelerated cement hydration and increased strength due to densification of the bulk matrix [37–39]. Various experiments on electrical curing and application of the so-called "maturity method" approach [15] for cement-based materials have been performed and reported [40–44]. The major outcome from these studies is mainly related to prediction of long-term mechanical properties (e.g. strength) and thermal conditions (e.g. heat development) from short-term tests and derived sets of experimental data.

Considering the above relationships, the objective of this work was to evaluate the effect of stray current on the mechanical and electrical properties of 28-days cured mortar in two very distinct exposure conditions (sealed and water-submerged). The motivation for these studies was in view of two main points. Firstly, stray current effects on reinforced concrete structures are mainly considered and reported with respect to steel corrosion, although reported loss of bond strength, coarsening of the pore network, etc. are among effects related to the cement-based material itself [27, 39, 45]. In other words, steel corrosion is well recognised as a consequence of stray current, while the mechanical and electrical properties of the cement-based bulk material are not considered to be subject to change and rather neglected in the present state-of-the-art. Therefore this aspect was studied in this work.

Secondly, if environmental conditions are taken into account, the presence of concentration gradients (e.g. as in underground structures or water-submerged conditions) or the absence of such (e.g. the bulk concrete in large structures, as in sealed conditions) would determine different level of material development in conditions of stray current. In these conditions, ion and water transport are determined by both diffusion and migration. However, in the former case (concentration gradients present), leaching-out would also be relevant and depend on the current density levels to a large extent. In the latter case (no concentration gradient) the effect of stray current would be expressed only in enhanced internal ion and water transport, potentially resulting in altered cement hydration due to migration-controlled phenomena. Therefore, evaluation of material properties in sealed conditions, will explicitly reflect the effect of stray current, when no ion or water exchange with external medium are relevant. In contrast, the development of material properties in water-submerged conditions would reflect the effect of stray current on both ion and water diffusion and migration, together with the contribution of leaching-out effects.

In view of the above and with regard long-term behaviour of cement-based materials in conditions of stray current, the ageing factors and apparent diffusion coefficients were also derived for sealed conditions, based on experimentally recorded electrical resistivity and implementing the above discussed and reported relationships. These were linked to the effect of stray current, rather than derived as absolute values or for the purpose of service life predictions. The outcomes were compared to the relevant control cases and used to evaluate the overall performance of cement-based materials, when ion and water migration contribute to diffusion-controlled transport mechanisms.

4.3 Experimental Materials and Methods

4.3.1 Materials

Mortar cubes of 40 mm × 40 mm × 40 mm (Fig. 4.1) were cast, using OPC CEM I 42.5 N with w/c ratio of 0.5 and 0.35. The cement-to-sand ratio used was 1:3. The chemical composition (in wt. %) of CEM I 42.5 N (ENCI, NL) is as follows: 63.9% CaO; 20.6% SiO_2; 5.01% Al_2O_3; 3.25% Fe_2O_3; 2.68% SO_3; 0.65% K_2O; 0.3% Na_2O. After casting and prior to conditioning, the specimens were cured in a fog-room of 98% RH, at 20 °C for 28 days; after de-molding, electrical connections were made to apply electrical current through cast-in electrodes (metal plates) on the two opposite sides of each cube (Figs. 4.1 and 4.4). The electrodes also served the purpose of measuring electrical resistivity (Figs. 4.1 and 4.4). For sealed conditions, the mortar specimens were sealed with bee wax to prevent water evaporation. For water-submerged conditions, identical specimens were submerged in water-containing vessels throughout the test.

4.3.2 Sample Designation and Current Regimes

The mortar specimens were cast in two main groups, differing in w/c ratio, i.e., 0.35 and 0.5. These two specimens' groups were presented by three subgroups: (1) control group – no DC current involved; (2) group "100 mA/m^2" and (3) group "1 A/m^2", where DC current was relevant at the respective current levels.

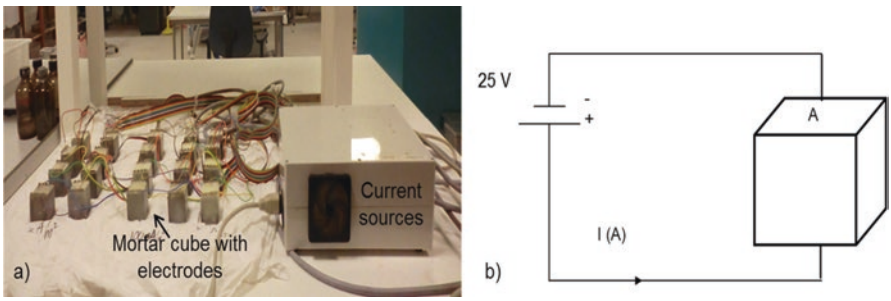

Fig. 4.4 (**a**) Experimental setup (sealed condition) for mortar cubes of w/c ratio 0.5 and 0.35; **(b)** schematic representation for electrical current application through surface area A of the mortar specimens

4.3.3 Methods

4.3.3.1 Mortar Electrical Resistivity

The electrical resistivity of the mortar cubes was measured using an alternating DC 2-pin method [27], where the "pins" are the metal electrodes (plates) with dimensions equal to the sides A of the mortar cubes, Fig. 4.4. To avoid polarisation effects during measurement for the water-submerged groups, the mortar cubes were taken out from the medium and cloth dried prior to testing. The resistance was measured by applying an alternating DC current of 1mA at a frequency of 1 kHz. An R-meter was used to record the electrical resistance of the mortar. For the "under current" regime (groups 100 mA/m^2 and 1 A/m^2), the resistance measurements were performed after current interruption of approximately 30 min. The electrical resistivity was calculated using Ohm's Law based on two probes measurements (as previously introduced in the Sect. 4.2.2).

4.3.3.2 Compressive Strength

Standard compressive strength tests were performed on the 40 mm × 40 mm × 40 mm mortar cubes at the hydration age of 28 days as initial measurement and later on after 3, 7, 14, 56, and 84 days of conditioning (i.e., 31, 42, 84, and 112 days of age). Three replicate mortar specimens were taken out from the conditioning setup and tested within a 5-min time interval.

4.4 Results and Discussion

4.4.1 Compressive Strength

Global mechanical properties of cement-based materials are of importance for the assessment of overall performance. In order to evaluate the influence of stray current flow on mechanical properties, compressive strength was recorded. Figure 4.5 shows the strength development of the 28-day cured mortar specimens of w/c ratio 0.5 and 0.35 in sealed and water submerged conditions. As expected, compressive strength increases with time and within cement hydration, which was relevant for all groups. The effect of w/c ratio can be clearly observed i.e. the specimens with w/c ratio of 0.35 presented higher compressive strength compared to those of w/c ratio 0.5, irrespective of exposure conditions and stray current effects. This trend of performance is well known and is generally due to a larger capillary porosity in the former case and a denser microstructure in the latter case [42].

The effect of electrical current in sealed conditions is more obvious at later stages – after 56 days, where stabilisation of compressive strength for control cases was observed, whereas a still gradual increase was relevant for the "under current"

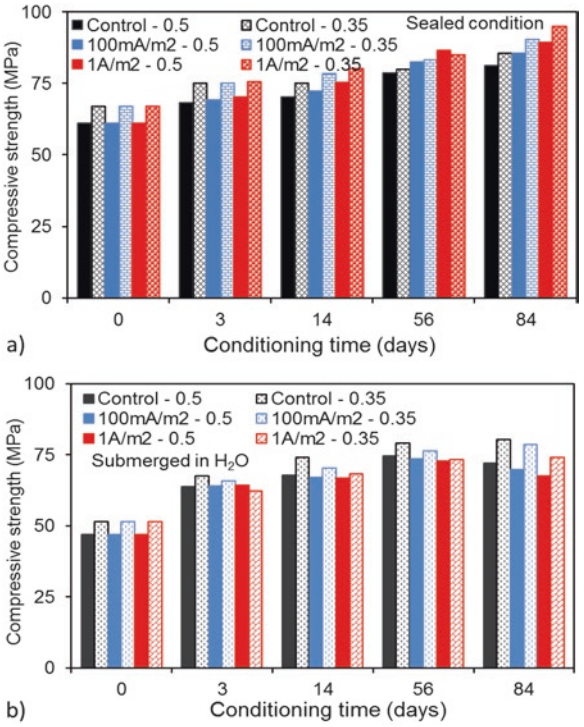

Fig. 4.5 Compressive strength of 28-day cured mortar specimens of w/c 0.35 and 0.5 as a function of hydration age in: **(a)** sealed conditions; **(b)** fully submerged in water conditions

regimes. Increased compressive strength at the end of the test was especially relevant for the 1A/m^2 group at w/c ratio of 0.35 (Fig. 4.5a). This is a result of enhanced cement hydration at lower pore water content, leading to a more pronounced development of a rigid microstructure, if all these are compared to w/c ratio of 0.5 and control conditions.

In contrast to the sealed conditions, the compressive strength of water-submerged mortar decreased as a result of stray current (Fig. 4.5b). This was more pronounced towards the end of the test. Calcium ions leaching-out would result in depreciation of mechanical performance due to microstructural changes. This outcome is consistent with previous results on partly submerged in water specimens, where chemical analysis of the external medium, together with microstructural analysis supported the observed evolution of mechanical properties [27]. The effect of w/c ratio and stray current can be judged in parallel by comparing the difference in compressive strength between the specimens "under current" and the relevant control cases at identical age. Similarly to the sealed conditions, although with a reversed trend, the highest current density level resulted in the largest effect at the end of the test i.e. the lowest compressive strength for both w/c ratio 0.35 and 0.5 were recorded for mortar subjected to stray current of 1 A/m^2.

The trend of compressive strength development of the hereby tested mortar specimens at early and later stages is well in line with the development of electrical resistivity, as presented and discussed in what follows.

4.4.2 Electrical Resistivity

Electrical resistivity is a rapid and nondestructive testing method that provides an indication for the quality of concrete structures. The electrical resistivity of concrete can be also defined as the resistance of the matrix to water and aggressive ions penetration. It could also be an indication of properties development, when water and ion transport due to migration are concerned, e.g., when electrical current flows through a unit length or a unit cross-section of a concrete specimen.

The electrical current is "carried" by ionic charge, flowing through the concrete pore solution. Hence, water and ions migration in conditions of current flow will be involved in addition to diffusion-controlled transport (absorption or capillary suction are not considered). Enhanced ion and water flow would result in enhancement, or at least alteration, of cement hydration. Additionally, leaching-out for water-conditioned specimens, would contribute to microstructural changes and potentially be reflected in changes in electrical properties. All these would affect the development of electrical resistivity in conditions of current flow, if compared to control conditions. Next, the electrical resistivity values are affected by several factors including different concrete mixture (e.g. binder/cement type, water to cement ratio, aggregates, pozzolanic admixtures) and environmental conditions (e.g. temperature, humidity) [46].

For this experiment, w/c ratio and exposure conditions were variables, all other factors were maintained identical. The effect of electrical current was recorded with respect to w/c ratio and external medium and compared to identical control specimens in each test series.

For the sealed specimens, the electrical resistivity gradually increased with time (Fig. 4.6). A close to linear relationship was observed with the level of current density, the highest values were recorded for the $1A/m^2$ regimes in both series of w/c ratios 0.35 and 0.5. As aforementioned, and as previously reported [27], this result is attributed to on-going cement hydration, minimized temperature loss and no interaction with external environment. Lower w/c ratio would additionally account for a denser microstructure and a reduction in the capillary pore volume of the mortar specimens. Therefore, the electrical resistivity values gradually increased with time due to the progress of cement hydration and subsequent development (densification) of the bulk microstructure.

Since the electrical current is carried by ionic flow through the pore solution of the mortar specimens, higher water/cement ratio results in an "easier" electrical current flow (i.e. low electrical resistance/resistivity). In contrast, the lower w/c ratio would impede electrical current flow (i.e. high electrical resistance/resistivity). If a correlation of factors is made e.g. w/c ratio and current flow effects on electrical properties of mortar, it is well seen that electrical resistivity increased for the specimens in conditions of electrical current, irrespective of the w/c ratio, Fig. 4.6c). In other words, for the specimen groups $100\ mA/m^2$ and $1A/m^2$, cement hydration was enhanced by elevated internal water and ion transport. This result in higher electrical resistivity over time – in the range of 480 to 530 Ohm.m, if compared to control conditions – approximately 350 Ohm.m towards the end of the test. Slightly higher

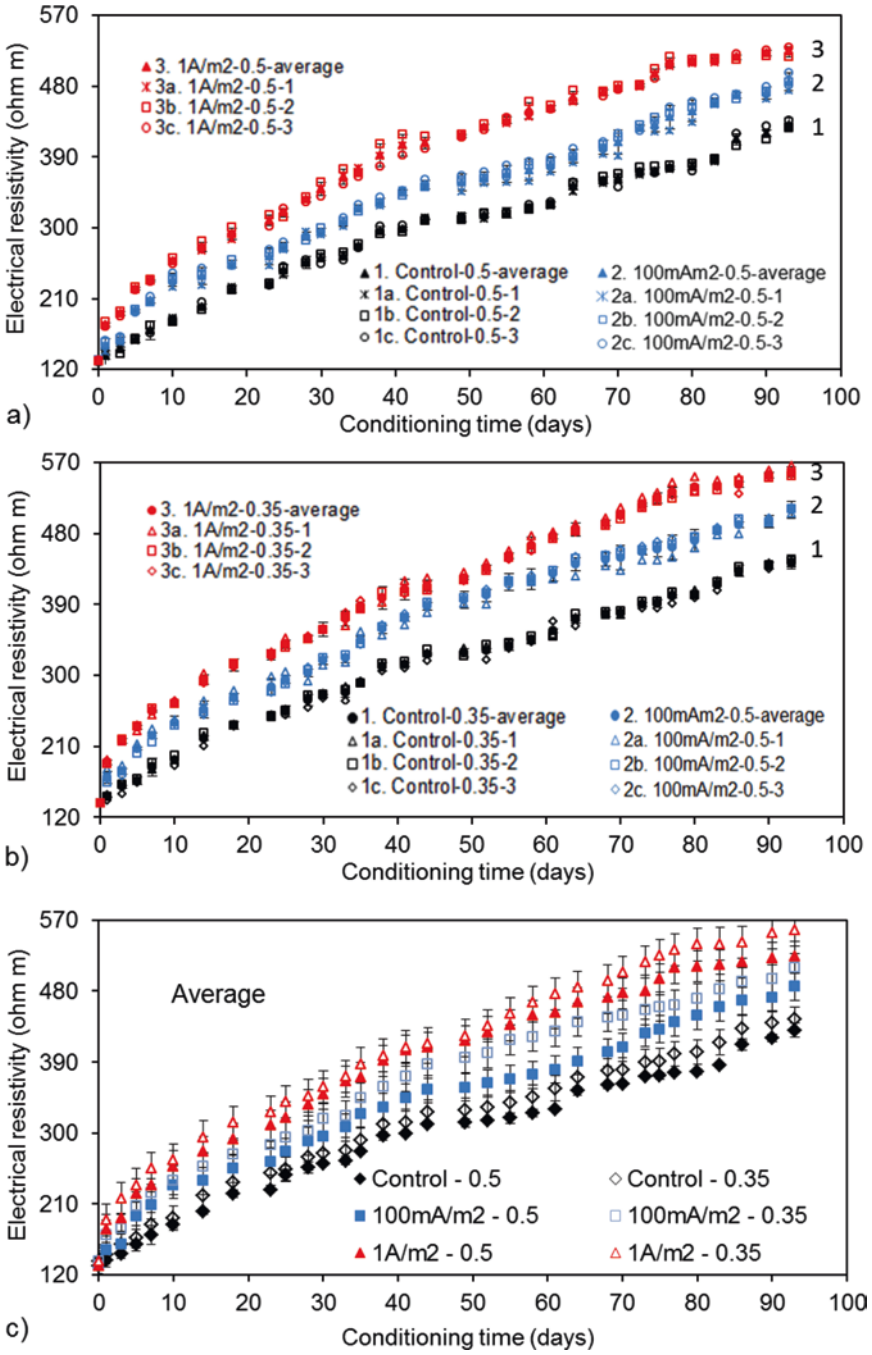

Fig. 4.6 Electrical resistivity values (3 replicates per group) of mortar specimens in sealed condition for w/c ratio 0.5 (**a**), w/c ratio 0.35 (**b**), and averaged data (**c**)

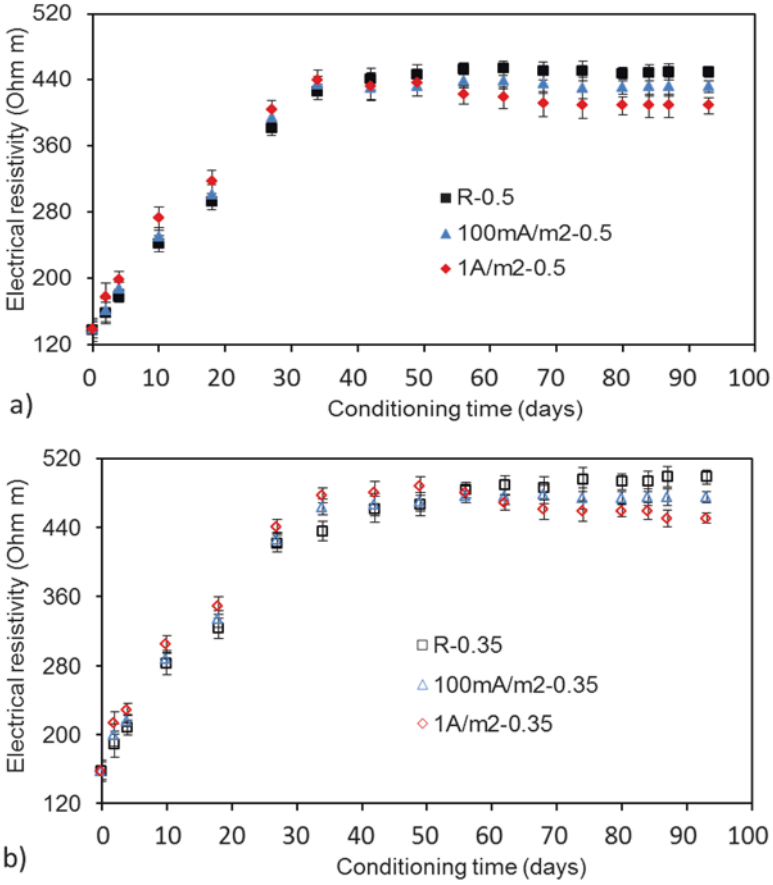

Fig. 4.7 Electrical resistivity of 28-day cured, water submerged mortar specimens of **(a)** w/c ratio 0.5 and **(b)** w/c ratio 0.35

values were recorded for the lower w/c ratio group (0.35) compared to the 0.5 w/c ratio group in both control and under current conditions (Fig. 4.6c), which was as expected and as previously discussed.

Figure 4.7 presents the evolution of electrical resistivity of the 28 days-cured mortar specimens, fully submerged in water. Similarly to sealed conditions, the effect of stray current was evaluated in parallel to the effect of varying w/c ratio and compared to control conditions of the same w/c ratio, i.e. w/c 0.5 (Fig. 4.7a) and w/c 0.35 (Fig. 4.7b). As can be observed, until ca. 40 days of conditioning (or ca. 70 days of age), the electrical resistivity for all specimens increased with time, irrespective of w/c ratio and conditions – Figs. 4.7a, b). This is logic and as expected, reflecting the maturity development of the cement matrix with time of hydration. After 40 to 55 days of conditioning, a subsequent increase and stabilization for the control specimens was recorded, but a decreasing trend for the "under current" conditions was observed. Increase or stabilization of electrical resistivity values

follows the logic of continuous cement hydration with time and conditioning. The decrease of electrical resistivity for the water-conditioned specimens after longer treatment (> 50 days), was obvious, especially if compared to sealed specimens (Fig. 4.6). This result is linked to leaching-out and re-distribution of the pore network, which are not subject to discussion in this work. Some of these effects were previously reported for partly submerged in water specimens [27]. This negative effect of stray current can be well observed in the water-submerged group, reflected by the lowest electrical resistivity for specimens, subjected to the highest current density levels (Fig. 4.7). As can be also observed in both Fig. 4.7a) and Fig. 4.7b), the negative effect of stray current was not determined by w/c ratio i.e. was relevant at comparable levels in both cases of w/c 0.35 and w/c 0.5, despite the lower amount of pore water at the w/c ratio of 0.35, compared to that of w/c ratio 0.5.

The results from electrical resistivity measurements are well in line with the recorded compressive strength in both sealed and water-submerged conditions (Fig. 4.5). Increasing electrical resistivity and higher compressive strength for sealed conditions were the result from stray current, where no concentration gradient with external medium was relevant. In contrast, decrease in electrical and mechanical properties was observed for water-treated specimens, more pronounced for the highest current density level of 1 A/m^2.

Following the above discussed experimental results and the outlined in Section 4.2. methodology, the ageing factor for sealed mortar in the hereby tested conditions was determined. Next, the apparent diffusion coefficients were calculated and results discussed in view of the effect of stray current on mortar specimens of different w/c ratio.

4.4.3 Ageing Factors Determination

The recorded electrical resistivity values, as presented in Figs. 4.6 and 4.7, were employed in Eq. (4.5), which through curve fitting was used to derive the exponents $\boldsymbol{q}$. The as derived exponent $\boldsymbol{q}$ values were later on used to calculate the ageing factors $\boldsymbol{n}$, following Eq. (4.6). Table 4.1 summarizes the obtained values for each group of specimens. An example of the fitting results for the sealed specimens are presented in Fig. 4.8 for w/c ratio 0.35 (Fig. 4.8a) and w/c ratio 0.5 (Fig. 4.8b). Curve fitting of Eq. (4.5) for water-submerged conditions was not possible, since on one hand the obtained error was very large and not presenting meaningful results. On the other hand, it is logic that the same function cannot be employed for two very

Table 4.1 Summarized $\boldsymbol{q}$ values and calculated aging factor $\boldsymbol{n}$ (Eq. 4.6) for mortar, cast from CEMI 42.5 N and cured for 28 days

	Sealed experiments – w/c 0.5			Sealed experiments – w/c 0.35		
Parameters	Control	100 mA/m^2	1 A/m^2	Control	100 mA/m^2	1 A/m^2
Values of $\boldsymbol{q}$	0.295	0.310	0.328	0.306	0.321	0.337
Aging factor ($\boldsymbol{n}$)	0.369	0.388	0.410	0.383	0.401	0.421

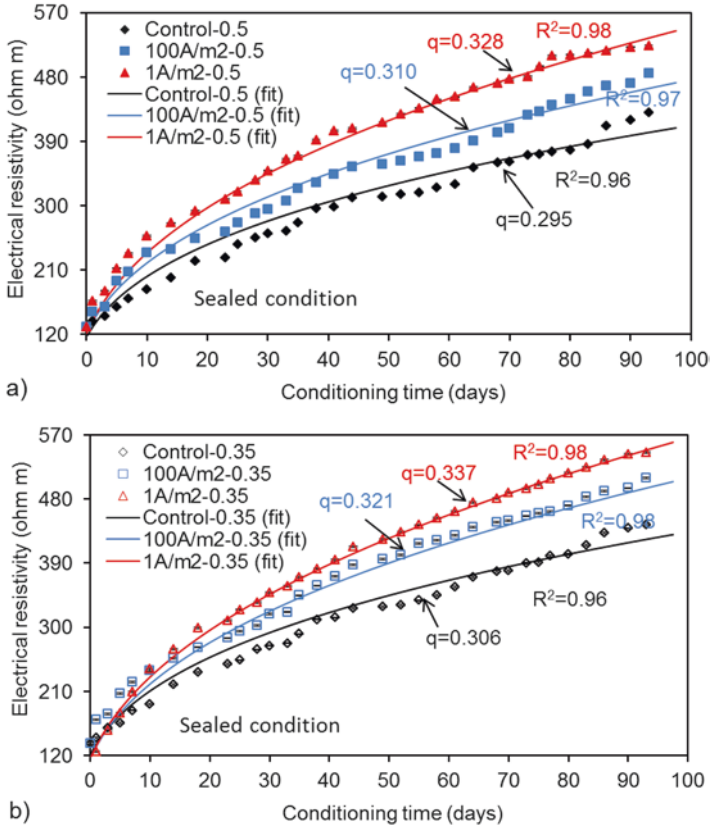

Fig. 4.8 Electrical resistivity values of mortar specimens in sealed condition and aging factor "***q***" obtained from fitting curve using Eq. (4.5) with w/c ratio 0.5 (**a**) and w/c ratio 0.35 (**b**)

different exposure conditions. Therefore, the application of the reported in literature analytical approaches for ageing factors determination, based on electrical resistivity, were only applied to the sealed specimens in this work.

As seen in the Fig. 4.8, the exponent ***q***values increased with increasing the level of electrical current for both w/c ratio 0.5 and 0.35. The exponent ***q*** values for control conditions was in the range of 0.369 - 0.383, while for the 100 mA/m^2 and $1A/m^2$ groups a range of 0.388 - 0.421 was recorded. It was also recorded that the exponent ***q*** values for the mortar groups of w/c ratio 0.35 was slightly higher than that, derived for w/c ratio 0.5. Although the difference was not significant, the result can be attributed to a potentially more pronounced effect on cement hydration, and a more substantial pore refinement for the mortar specimens of w/c ratio 0.35 (lower amount of capillary water initially present if compared to w/c ratio 0.5) resulting in increase of electrical resistivity. Additionally, lower w/c ratio tends to result in higher electrical resistivity due to a lower content of the liquid phase.

Table 4.1 summaries exponent ***q*** values as derived from the electrical resistivity records and the ageing factor ***n*** as calculated from the relationship between the exponent ***q*** and ***n***, using Eq. (4.6). From Eq. (4.6) it can be deduced that the exponent ***q***, derived from resistivity is slightly lower than ***n***, ***n*** obtained from diffusion coefficient. This is due to the fact that both electrical resistivity (ρ) and apparent diffusion coefficient (D_{ap}) evolve differently with time [17, 36]. Among other phenomena, the values of electrical resistivity (ρ), represent the evolution of microstructural properties (i.e. pore network and its connectivity) due to cement hydration and/or reactions with pozzolanic material, mineral admixtures, etc. Electrical resistivity changes can reflect variation in diffusion coefficients as well, since diffusivity is determined by microstructure development, including chloride binding capacity in the bulk matrix. The diffusion coefficient Dap, however, also reflects the surface chloride binding and chloride surface concentration with time. Although the difference between ***q*** and ***n*** values (Table 4.1) was not well pronounced, the variation of derived values can be attributed to the influence of stray current on ions and water migration. These in turn affect microstructural development and the evolution of mechanical and electrical properties, respectively.

As seen in the Table 4.1, both ***n*** and ***q*** values changed with water-to-cement ratio and the level of stray current flow. As expected, the aging factor ***n*** increased with decreasing of water-to-cement ratio and with increasing electrical resistivity values. As aforementioned, lower water-to-cement ratio results in higher electrical resistivity, as stated by MacDonald and Northwood [47], and the variation of electrical resistivity is caused by changing in porosity, determined by water content and the water-to-cement ratio.

For the experimental conditions of this work, the aging factor was obviously not only depending on the w/c ratio, but was also affected by the stray current flow. The simultaneous effect of stray current flow and water-to-cement ratio can be deduced from the results in Table 4.1. It can be seen that the aging factor increased with increasing the level of stray current flow for both w/c ratio 0.5 and 0.35. The aging factor for specimens of w/c ratio 0.35 tends to have higher values than that for specimens of w/c ratio 0.5. At lower w/c ratio, the stray current flow had a larger effect in view of increasing the temperature of a lower amount of pore water. As a consequence, the rate of cement hydration increased faster for specimens of w/c ratio 0.35, compared to these of w/c ratio 0.5. This in turn led to a more rapid pore refinement, or densification of cement bulk matrix, in specimens of w/c 0.35. However, if control and under current conditions are compared within the groups of same w/c ratio (Table 4.1), the following can be observed: compared to control conditions, the aging factor increased with 5.1% and 11.1% at the level of current densities 100 mA/m^2 and 1 A/m^2, respectively, for the groups of w/c ratio 0.5. In contrast, for the groups of w/c ratio 0.35, the aging factor increased with about 4.7% and 10% at the current density levels of 100 mA/m^2 and 1 A/m^2. Although the overall aging factor for w/c ratio 0.35 was slightly higher than that for w/c ratio 0.5, the stray current flow contributed to the aging factor changes to a higher extent at w/c ratio 0.5, if under current regimes are compared to control conditions in one and the same w/c ratio group.

Table 4.2 Aging factor n for OPC mixtures from literatures

w/c	***n***-values	References
0.5	0.320	Stanish [48]
0.5	0.178	Zhuqing Yu [24]
0.45	0.264	Bamforth [23]
0.45	0.275, q = 0.22	Andrade [11]
0.45	0.236	Dalen [31]
0.45	0.182	Maes [49]
0.4	0.350	F. Presuel-Moreno [13]

The derived exponent ***q*** and ***n*** values in this study are well in line with values reported in the literature, especially if conditions similar to the hereby tested control series are considered [11, 22, 23]. As can be observed from Table 4.2 (e.g. ref. [11] and [48] refer to sealed conditions, ref. [13] – to immersed, ref. [23] – to splash zone, ref. [24] – to lab), the ageing factor (n) determined by both electrical resistivity-based and diffusion coefficient-based approach as previously reported, are in the range of the hereby derived ones (Table 4.1). This outcome denotes for a valid approach towards retrieving reliable results for the present investigation, on one hand. On the other hand, the effect of stray current on ageing factors and maturity level of cement-based materials is apparently possible to be quali- and quantified following the same approach.

4.4.4 Diffusion Coefficient

By considering the previously introduced theoretical background and employing the aging factor ***n*** as presented in the Table 4.1, the apparent diffusion coefficient as function of time can be predicted, using Eq. (4.3). Graphically this is presented in Figs. 4.9 and 4.10. Figure 4.9 depicts a comparison of the apparent diffusion coefficient (D_{ap}) as derived from the obtained aging factors ***n*** in this study (curve "control 0.5") and D_{ap} as reported in literature for control conditions. As seen in the Fig. 4.9, there is a good agreement between the D_{ap} values, predicted based on calculation from the aging factor ***n*** and these derived from direct measurements of apparent diffusion coefficient. This outcome can be further used to predict the influence of stray current flow on apparent diffusion coefficient of cement-based materials. Figure 4.10 depicts the evolution of D_{ap} for the under current subgroups 100 mA/m^2 and 1 A/m^2 in comparison to the control group in this study. As expected, the apparent diffusion coefficient did not change significantly at early stages, which holds for both groups of w/c ratio of 0.5 and 0.35. A gradual decrease, however, was observed at later stages with decreasing the w/c ratio (i.e., D_{ap} of w/c ratio 0.35 is lower than that of w/c ratio 0.5).

As far as the effect of stray current is concerned, in both groups of w/c ratios of 0.35 and 0.50, a decrease of D_{ap} was observed over time as an indirect effect of the stray current. This was significantly more pronounced for the higher current density group (1 A/m^2) in combination with lower w/c ratio (0.35).

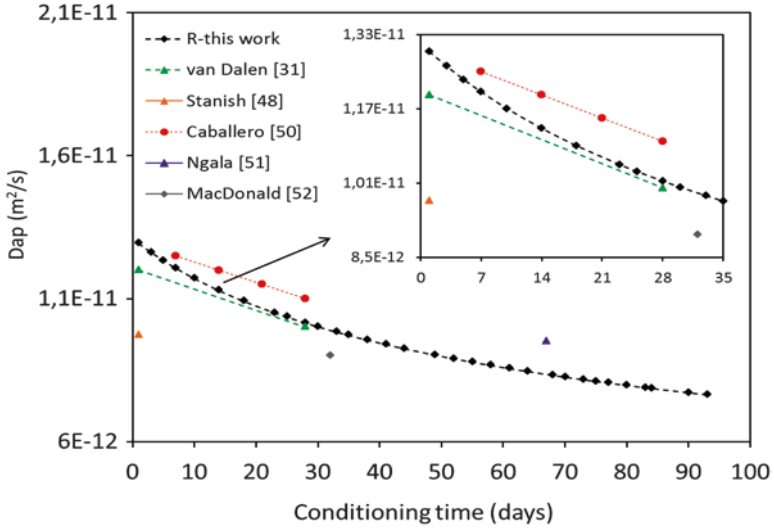

Fig. 4.9 Prediction of apparent diffusion coefficient calculated using Eq. (4.3) based on aging factor (***n***), as derived from electrical resistivity records, compared to reported literature results

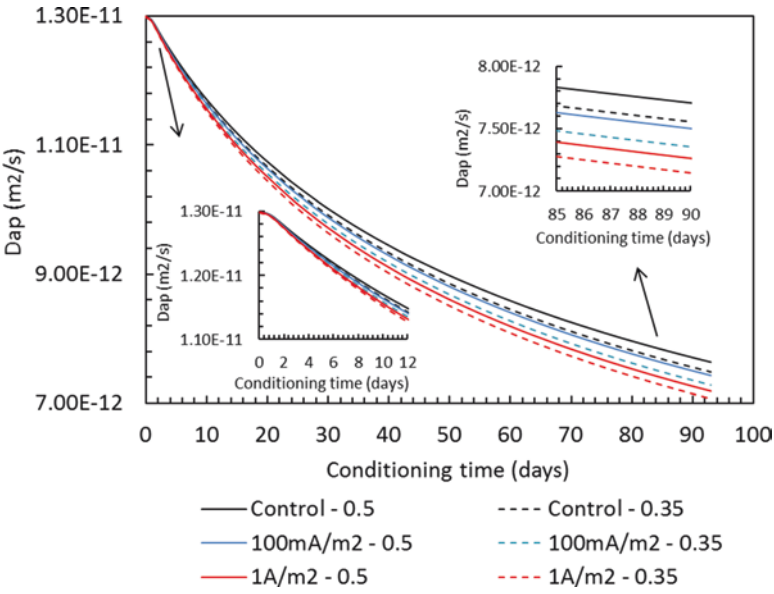

Fig. 4.10 Apparent diffusion coefficient of mortar specimens subject to stray current flow calculated using Eq. (4.3) based on aging factor (***n***) derived from electrical resistivity records

Obviously, the different levels of stray current density and w/c ratio – as separately evaluated and as a synergetic effect – exert influence on the maturity levels and aging factors of cement-based materials. Electrical resistivity values can be used as an alternative of diffusion coefficients within the determination of the aging factor of cement-based materials. Moreover, the obtained results, using this alternative approach, are in a very good agreement with results, where values from chloride diffusion tests were used.

In a "reversed" approach, the aging factors, as derived based on electrical resistivity, can be used to determine diffusion coefficients and predict the development of apparent chloride diffusivity. This approach can be used further to predict service life of cement-based materials due to stray current flow. This study discussed only relatively lower levels of current flow, which result in positive effects, e.g., densification of the bulk matrix, increased compressive strength. Should be noted that in practical situations, this is not necessarily the case and the level of stray current can be significant and leading to negative side effects. For example, if combined with environmental conditions as level of humidity and chloride content, stray current can cause leaching out of calcium-baring phases and reduced global properties and performance would be relevant. This is especially the case when enhanced water and ion migration are involved, as within electrical current flow through a cement-based matrix.

Therefore, further research is necessary in order to define a threshold value for positive and/or negative effects of electrical current flow (stray current respectively) on cement-based material properties and performance within service life. In the following section, the concept of applying the above considerations to (potentially practical) cases of significantly larger current density levels is outlined. Also presented is an example for the negative effect of stray current in relevant environmental conditions and in view of aging factors determination.

4.5 Conclusions

This chapter discussed the influence of stray current flow on material properties and performance of 28-day cured cement-based materials in two distinct environmental conditions. The ageing factor, as a parameter linked to durability of cement-based materials, was determined from electrical resistivity development for sealed conditions. Based on the experimental results and analytical approach, the following conclusions can be drawn:

The ageing factor for control specimens in sealed conditions, obtained from electrical resistivity development over time, was in the range of those published by other researchers. This indicates that this method is potentially reliable and can be applied also to determine the influence of stray current flow on cement-based materials. The results show that the influence of stray current not only depends on the level of current flow, but is also largely determined by the relevant environmental conditions.

In sealed conditions, the ageing factor (n) obtained from electrical resistivity increased with the level of stray current flow and with lowering the w/c ratio, as

also indicated by increase in compressive strength development. The ageing factor for water-submerged specimens was not possible to be determined using the same approach. However, the real experimental data shows the negative effect of stray current in view of decreased electrical properties and mechanical performance.

The approach to determine the ageing factor from electrical resistivity development may be useful to determine the apparent diffusion coefficient of cement based materials to a certain extent and in controlled environment. Deriving ageing factors for various exposure conditions, however, needs to consider other factors and materials development over time. The hereby discussed analytical functions were found to be not directly applicable for water-submerged specimens in view of the effects of stray current.

Acknowledgements The financial support from Directorate General of Higher Education Ministry of Education Republic of Indonesia is gratefully acknowledged. The authors would like to thank technicians of Microlab, Section of Material and Environment, Delft University of Technology for supporting an experimental setup.

References

1. Audenaert K, Yuan Q, de Schutter G (2010) On the time dependency of the chloride migration coefficient in concrete. Constr Build Mater 24(3):396–402
2. Tang L (1999) Concentration dependence of diffusion and migration of chloride ions: Part 2. Experimental evaluations. Cem Concr Res 29(9):1469–1474
3. Tang L, Gulikers J (2007) On the mathematics of time-dependent apparent chloride diffusion coefficient in concrete. Cem Concr Res 37(4):589–595
4. Tang L, Nilsson LO (2004) On relationships between different chloride diffusion and/or migration coefficients in concrete. In: Proceedings of the 3rd RILEM workshop on testing and modelling the chloride ingress into concrete. RILEM Publications Sarl, Bagneux, pp 317–328
5. Yuan Q, De Schutter G, Shi C, Audenaert K (2008) The relationship between chloride diffusion and migration coefficients in concrete. In: 1st international conference on microstructure related durability of cementitious composites, 13–15 Oct 2008, Nanjing
6. Mingzhong Z (2013) Multiscale lattice Boltzman-finite element modelling of transport properties in cement-based materials. PhD thesis, Delft University of Technology
7. NORDTEST NT BUILD 443 (1995) Accelerated chloride penetration, Finland
8. NORDTEST NT BUILD 492 (1999) Chloride migration coefficient from non-steady state migration experiments, Finland
9. NORDTEST NT BUILD 355 (1997) Chloride diffusion coefficient from migration cell experi ments, Finland
10. Mangat P, Molloy B (1994) Prediction of long term chloride concentration in concrete. Mater Struct 27(6):338–346
11. Andrade C, Castellote M, d'Andrea R (2011) Chloride aging factor of concrete measured by means of resistivity. Proceedings of the XII-international conference on durability of building materials and components, Porto
12. Andrade C, Castellote M, d'Andrea R (2011) Measurement of ageing effect on chloride diffusion coefficients in cementitious matrices. J Nucl Mater 412:209–216
13. Presuel-Moreno F, Wu Y-Y, Liu Y (2013) Effect of curing regime on concrete resistivity and aging factor over time. Constr Build Mater 48:874–882

14. Millard SG, Gowers KR (1992) Resistivity assessment of in-situ concrete: the influence of conductive and resistive surface layers. Proc Inst Civil Eng Struct Build 94(4):389–396
15. Brooks AG, Schindler AK, Barnes RW (2007) Maturity method evaluated for various cementitious materials. J Mater Civ Eng 19:1017–1025
16. Bentz DP, Garboczi EJ (1999) Effects of cement particle size distribution on performance properties of Portland cement-based materials. Cem Concr Res 29(10):1663–1671
17. Brown PW, Dex S, Skalny JP (1993) Porosity/permeability relationships. Parts of 'Concrete microstructure porosity and permeability'. Roy DM, Brown PW, Shi D, Scheetz BE, May W. Strategic Highway Research Program, National Research Council, Washington, DC 1993. SHRP-C-628
18. Tang L, Nilsson LO (1992) Chloride diffusivity in high strength concrete at different ages. Nor Concr Res 11(1):162–171
19. Maage M, Helland S, Poulsen E, Vennesland O, Carlsen JE (1996) Service life prediction of existing concrete structures exposed to marine environment. ACI Mater J 93(6):602–608
20. Gulikers J (2006) Pitfalls and practical limitation in probabilistic service life modeling of reinforced concrete structures. In: Proceedings of the Eurocorr 2006, Maastricht 25–28 Sept 2006
21. Castellote M, Andrade C, d'Andréa R (2009) The use of resistivity for measuring aging of chloride diffusion coefficient. In: Proceedings RILEM TC 211-PAE international conference – concrete in aggressive aqueous environments, Toulose
22. Gehlen C (2000) Probabilistische Lebensdauerbemessung von Stahlbetonbauwerken, Dafst 510. Beuth Verlag, Berlin
23. Bamforth PB (1999) The derivation of input data for modelling chloride ingress from eight year UK coastal exposure trials. Mag Concr Res 51(2):87–96
24. Yu Z (2015) Microstructure development and transport properties of Portland cement-fly ash binary systems – in view of service life predictions. PhD thesis, Delft University of Technology, Delft
25. DuraCrete (2000) Probabilistic performance based durability design of concrete structures. Contract BRPR-CT95–0132, Project BE95–1347. Document BE95–1347/R17
26. CUR-Bouw&Infra (2009) Duurzaamheid van constructief beton met betrekking tot chloride-geïnitieerde wapeningscorrosie – Leidraad voor het formuleren van prestatie-eisen-Achtergrondrapport (in Dutch), Tu Delft, 19 Mei 2009
27. Susanto A, Koleva DA, Copuroglu O, van Beek C, van Breugel K (2013) Mechanical, electrical and microstructural properties of cement-based materials in conditions of stray current flow. J Adv Concr Technol 11(3):119–134
28. Andrade C., d'Andrea R. Electrical resistivity as microstructural parameters for the modelling of service life of reinforced concrete structures, 2nd international symposium on Service Life Design for Infrastructure, October 2010, Delft, RILEM proceedings
29. Singh Y (2013) Electrical resistivity measurements: a review. Int J Mod Phys Conf Series 22:745–756
30. Wenner F (1915) A method for measuring earth resistivity. Bull Bureau Stand 12:469–478
31. van Dalen Sander M (2005) Experimenteel onderzoek naar de RCM-methode (In Dutch). Master thesis, Delft University of Technology
32. Naish CC, Harker A, Carney RFA (1990) Concrete inspection: interpretation of potential and resistivity measurements. In: Page CL, Treadaway KWJ, Bamforth PF (eds) Corrosion of reinforcement in concrete. SCI, London, pp 314–332
33. Millard SG (1991) Reinforced concrete resistivity measurement techniques. Proc Inst Civil Eng 2:71–88
34. Telford WM, Telford WM, Geldart LP, Sheriff RE (1990) Applied geophysics. Cambridge University Press, New York
35. Polder R, Andrade C, Elsener B, Vennesland O, Gulikers J, Weidert R, Raupach M (2000) Rilem TC 154-EMC: electrochemical techniques for measuring metallic corrosion – test methods for on site measurement of resistivity of concrete. Mater Struct Mater Constr 33:603–611
36. Feliu S, Andrade C, Gonzalez JA, Alonso C (1996) A new method for in situ measurement of electrical resistivity of reinforced concrete. Mater Struct 29:362–365

37. Susanto A, Koleva DA, van Breugel K (2015) The effect of temperature rise on microstructural properties of cement-based materials: correlation of experimental data and a simulation approach. In: Mori G, Hribernik B, Stellnberger KH, Dworak Y (eds) Proceeding of the European corrosion congress, EUROCORR 2015 (pp 1–10). s.l.: European Federation of Corrosion
38. Susanto A, Koleva DA, van Breugel K, Koenders EAB (2014) Modelling the effect of electrical current flow on the hydration process of cement-based materials. In: Mangabhai RJ, Bai Y, Goodier CI (eds) Extended abstract: young researchers' forum II: construction materials. University College London, London, pp 41–48
39. Susanto A, Koleva DA, van Breugel K (2014) Altered cement hydration and subsequently modified porosity, permeability and compressive strength of mortar specimens due to the influence of electrical current. In: Lazzari L, Fedrizzi L, Mol A (eds) Proceedings of the European corrosion congress (EUROCORR 2014). European Federation of Corrosion, Oxford, pp 1–10
40. Heritage I (2001) Direct electric curing of mortar and concrete. Napier University, Edinburgh
41. Bredenkamp S, Kruger D, Bredenkamp GL (1993) Direct electric curing of concrete. Mag Concr Res 45(162):71–74
42. Brooks AG, Schindler AK, Barnes RW (2007) Maturity method evaluated for various cementitious materials. J Mater Civ Eng 19:1017–1025
43. Abdel-Jawad YA (2006) The maturity method: Modifications to improve estimation of concrete strength at later ages. Constr Build Mater 20:893–900
44. Wilson JG, Gupta NK (2004) Equipment for the investigation of the accelerated curing of concrete using direct electrical conduction. Measurement 35:243–250
45. Susanto A, Koleva DA, van Breugel K (2014) DC current-induced curing and ageing phenomena in cement-based materials. In: van Breugel K, Koenders EAB (eds) Proceedings of the 1st international conference on ageing of materials and structures, AMS'14 (pp 562–568), 26–28 May 2014, Delft
46. Sengul O (2013) Factors affecting the electrical resistivity of concrete, Nondestructive Testing of Materials and Structures, RILEM Bookseries 6, doi 10.1007/978–94–007-0723-8-38, © RILEM 2013
47. MacDonald, K. A., and Northwood, D. O., Rapid estimation of water-cementitious ratio and chloride ion diffusivity in hardened and plastic concrete by resistivity measurement, S-P-191, M. S. Khan, American Concrete Institute, Farmington Hills, 1999, pp 57–68.
48. Stanish K, Thomas M (2003) The use of bulk diffusion tests to establish time-dependent concrete chloride diffusion coefficients. Cem Concr Res 33:55–62
49. Maes M, Caspeele R, Van den Heede P, De Belie N (2013) Influence of sulphates on chloride diffusion and the effect of this on service life prediction of concrete in a submerged marine environment. In: Strauss A, et al Life-cycle and sustainability of civil infrastructure systems proceedings of the third international symposium on life-cycle civil engineering (IALCCE'12), Vienna, 3–6 Oct, 2012. pp 899–906
50. Caballero J, Polder RB, Leegwater GA, Fraaij ALA (2012) Chloride penetration into cementitious mortar at early age. Heron 57(3):185–196
51. Ngala VT, Page CL, Parrott LJ, Yu SW (1995) Diffusion in cementitious materials: II further investigations of chloride and oxygen diffusion in well-cured OPC and OPC/30%PFA pastes. Cem Concr Res 25(4):819–826
52. MacDonald KA, Northwood DO (1995) Experimental measurements of chloride ion diffusion rates using a two-compartment diffusion cell: effects of material and test variables. Cem Concr Res 25(7):1407–1416